(12)

NWC TP 6205

Atmospheric Visibility Measurements at China Lake: A 5-Year Nephelometry Summary

by
A. Raymond Kelso
Public Works Department

JULY 1981

NAVAL WEAPONS CENTER
CHINA LAKE, CALIFORNIA 93555

Approved for public release; distribution unlimited

Naval Weapons Center
AN ACTIVITY OF THE NAVAL MATERIAL COMMAND

FOREWORD

This report presents preliminary results of a 5-year visibility measurement program conducted at the Naval Weapons Center. The work was performed during the period October 1975 through September 1980 and since 1977 has been funded by Public Works overhead funds.

This report was reviewed for technical accuracy by Paul R. Owens of the Electronic Warfare Department.

Approved by
J. L. HORACEK
Capt. U.S. Navy
Public Works Officer
25 June 1981

Under authority of
J. J. LAHR
Capt. U.S. Navy
Commander

Released for publication by
R. M. HILLYER
Technical Director

NWC Technical Publication 6205

Published by ..... **Technical Information Department**
Collation ..... **Cover, 20 leaves**
First printing ..... **175 Unnumbered copies**

UNCLASSIFIED

SECURITY CLASSIFICATION OF THIS PAGE (When Data Entered)

REPORT DOCUMENTATION PAGE		READ INSTRUCTIONS BEFORE COMPLETING FORM
1. REPORT NUMBER NWC TP 6205	2. GOVT ACCESSION NO. AD-A116 794	3. RECIPIENT'S CATALOG NUMBER
4. TITLE (and Subtitle) ATMOSPHERIC VISIBILITY MEASUREMENTS AT CHINA LAKE: A 5-YEAR NEPHELOMETRY SUMMARY		5. TYPE OF REPORT & PERIOD COVERED SUMMARY REPORT OCT 1975 - SEPT 1980
		6. PERFORMING ORG. REPORT NUMBER
7. AUTHOR(s) A. Raymond Kelso		8. CONTRACT OR GRANT NUMBER(s)
9. PERFORMING ORGANIZATION NAME AND ADDRESS Naval Weapons Center China Lake, Calif. 93555		10. PROGRAM ELEMENT, PROJECT, TASK AREA & WORK UNIT NUMBERS
11. CONTROLLING OFFICE NAME AND ADDRESS Naval Weapons Center China Lake, Calif. 93555		12. REPORT DATE July 1981
		13. NUMBER OF PAGES 38
14. MONITORING AGENCY NAME & ADDRESS(if different from Controlling Office)		15. SECURITY CLASS. (of this report) UNCLASSIFIED
		15a. DECLASSIFICATION/DOWNGRADING SCHEDULE

16. DISTRIBUTION STATEMENT (of this Report)

Approved for public release; distribution unlimited.

17. DISTRIBUTION STATEMENT (of the abstract entered in Block 20, if different from Report)

18. SUPPLEMENTARY NOTES

19. KEY WORDS (Continue on reverse side if necessary and identify by block number)

Extinction coefficient
Nephelometry
Particle scattering measurements
Rayleigh scatter
Visibility
Visual range

20. ABSTRACT (Continue on reverse side if necessary and identify by block number)

See Back of Form.

DD FORM 1 JAN 73 1473 EDITION OF 1 NOV 65 IS OBSOLETE
S/N 0102-LF-014-6601

UNCLASSIFIED

SECURITY CLASSIFICATION OF THIS PAGE (When Data Entered)

(U) *Atmospheric Visibility Measurements at China Lake: A 5-Year Nephelometry Summary*, by A. Raymond Kelso. China Lake, Calif., Naval Weapons Center, July 1981. 38 pp. (NWC TP 6205, publication UNCLASSIFIED.)

(U) Visibility impairment directly affects the performance of optical data gathering instrumentation used at the Naval Weapons Center, China Lake, Calif. As weapons systems become more complex, test requirements push optical instrumentation systems to their limits. Any increased visibility degradation poses a serious problem for operations on NWC's ranges.

(U) In response to the interest in visibility, a monitoring program was initiated in 1975 to provide baseline nephelometry data and to establish usable theoretical relationships between light, eye, and the atmosphere that would permit calculations of visual range.

(U) A brief discussion is given of the atmosphere's ability to attenuate light, and the meteorological conditions that contribute to the concentration of suspended aerosols in the China Lake area are discussed.

(U) Analysis of the 5-year data base indicates that significant variations in visibility occur on an annual, seasonal, and diurnal basis. These data are presented in graphical form indicating periods of highest and lowest visibilities.

CONTENTS

ACKNOWLEDGMENT

The author gratefully acknowledges Paul R. Owens of the Electronic Warfare Department of NWC, who had the foresight and the fortitude to begin the nephelometry measurement program, for his assistance in organizing and reviewing the materials for this report.

INTRODUCTION

The issue of visibility in the Southwest is a common concern, not only to the public, but to the military as well.[1] It is a common opinion that visibility levels in the Southwest have deteriorated and that the growth in population and expanding fossil fuel usage will further degrade visibility.[2-4]

Visibility impairment directly affects the performance of optical data gathering instrumentation used at the Naval Weapons Center, China Lake, Calif. As weapons systems become more complex, test requirements push optical instrumentation systems to their limits. Any increased visibility degradation poses a serious problem for operations on NWC's ranges.[1]

In response to the interest in visiblity, a monitoring program was initiated in 1975 to provide baseline nephelometry data and to establish usable theoretical relationships between light, eye, and the atmosphere that would permit calculations of visual range.

Before proceeding further a minimal discussion on the attenuation of light by the atmosphere is in order. Visibility is here defined as visual range, and the two terms will be used interchangeably; visual range is defined as the greatest distance at which an observer can distinguish a contrast between an object and its background.

The human eye and its ability to detect contrasts between an object and its surroundings is fundamental to visibility. Particles and gases in the atmosphere reduce contrast, making distant objects less distinct. Particles (or aerosols) have the ability to scatter and absorb light; they can cause the appearance of haze, reduce the contrast between the object of interest and the background, and change the perceived color of the view. These concepts are more thoroughly explored in Appendix A.

[1] Naval Weapons Center. *Effects of Visibility on Range Operations at the Naval Weapons Center*, by Carl W. Koiner. China Lake, Calif., NWC, August 1979. (NWC TP 6119, publication UNCLASSIFIED.)

[2] Environmental Protection Agency. "The 1977 Clean Air Act: Prevention of Significant Air Quality Deterioration," *Federal Register*, Vol. 43, No. 118 (June 19, 1978).

[3] Environmental Protection Agency. *Visibility in the Southwest*, by J. Trijonis and K. Yuan. Research Triangle Park, N.C., EPA, April 1978. (EPA 600/3-78-039, publication UNCLASSIFIED.)

[4] California Air Resources Board. *Visibility in California*, by John Trijonis. Sacramento, Calif., July 1980. (TSC-PD-B612-3, publication UNCLASSIFIED.)

Visibility impairment is caused by the following interactions in the atmosphere:

1. Light scattering by molecules of air and by particles (aerosols) (mathematically stated as the scattering coefficient (b_{scat})).

2. Light absorption by gases and particles (aerosols) (mathematically stated as the absorption coefficent (b_{abs})).

3. The summation of the scattering coefficient (b_{scat}) and the absorption coefficient (b_{abs}) (mathematically defined as the extinction coefficient (b_{ext})).

$$b_{ext} = b_{scat} + b_{abs}$$

The extinction coefficient is determined by the scattering and absorption of light by particles and gases and varies with pollutant concentration and wavelength of light.

Figure 1a shows a light beam (such as from the sun) transmitted through the atmosphere. The intensity of the beam decreases with distance as light is absorbed and scattered away from the direction of the observer.

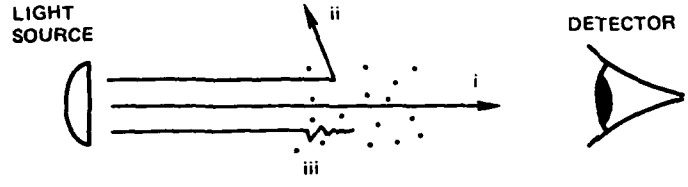

a. A schematic representation of atmospheric extinction, illustrating (i) transmitted, (ii) scattered, and (iii) absorbed light.

FIGURE 1. Daytime Visibility Limitations.[5]

Figure 1b demonstrates the basic principles of daytime visibility limitations. Just as a light beam is attenuated by the atmosphere, the light from the target to the observer is further diminished by scattering and absorption.

[5] Council of Environmental Quality. *Visiblity Protection for Class I Areas: The Technical Basis*, by Robert J. Charlson, Alan P. Waggoner, and John F. Thielke, University of Washington. Washington, D.C., August 1978. (Publication UNCLASSIFIED.)

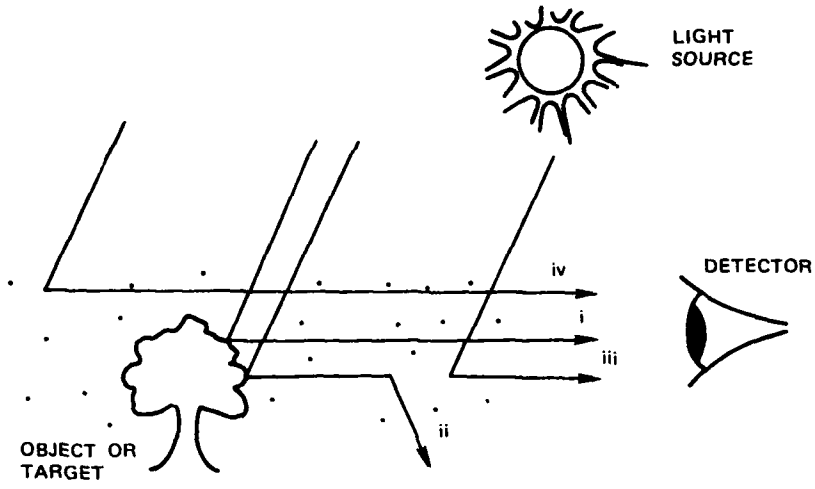

b. A schematic representation of daytime visibility, illustrating: (i) residual light from target reaching observer, (ii) light from target scattered out of observer's line of sight, (iii) airlight from intervening atmosphere, and (iv) airlight constituting horizon sky. (For simplicity, "diffuse" illumination from sky and surface is not shown.) The extinction of transmitted light attenuates the "signal" from the target at the same time as the scattering of airlight is increasing the background "noise."

FIGURE 1. (Contd.)

It is well known that the extinction coefficient, b_{ext}, is dominated by the scattering coefficient, b_{scat}.[3,5,6] With that fact in mind, the measurements program was designed around an instrument called the integrating nephelometer. The nephelometer measures the scattering of light due to particles in the atmosphere.

The scattering of light due to particles (b_{sp}) is only one part of the extinction coefficient; however b_{sp} is the major contributor to visibility impairment. By measuring b_{sp}, visual range can readily be estimated using known formulas. A more detailed discussion of visibility theory and visual range calculations can be found in Appendix A.

NEPHELOMETRY AND VISIBILITY MEASUREMENTS

"The aspect of the environment that is to be measured must be conceptualized and some means must be devised for representing that aspect to relevant observers."[6]

The integrating nephelometer was developed in 1943 as a simple means for measuring visual range, and the principle has been widely used.[5] Nephelometers are available

[6] Environmental Protection Agency. *Protecting Visibility-An EPA Report to Congress*, by Office of Air Quality Planning and Standards. Research Triangle Park, N.C., EPA, October 1979. (EPA-450/5-70-008, publication UNCLASSIFIED.)

commercially from both U. S. and foreign manufacturers, and various versions can be obtained that differ in sensitivity and wavelength response.*

TECHNICAL DESCRIPTION

The original instruments used by NWC were Meteorology Research, Inc. (MRI) Model 1560 Integrating Nephelometers. These instruments were later modified by Dr. A. P. Waggoner to keep up with state-of-the-art technology. The Model 1560 consists of two parts: the optical assembly and the blower box (Figure 2). The optical assembly contains the optical chamber, lamp assembly, and electronic circuitry. The blower box houses the sample blower, clean air pump, and power supply transformer. The two parts are connected by an air sample hose, clean air hose, and electrical cable.

As shown in Figure 3, the air sample is continuously drawn through an optical chamber by a blower. An opal glass diffuser allows a quartz halogen lamp to illuminate the optical chamber. The illuminated sample volume is defined by a series of diaphrams and the location of the light diffusing surface. The geometry was selected to provide an integrated value of the scattering coefficient over a relatively wide angle. A photomultiplier tube is located at one end of the optical chamber and "looks" at a light trap at the opposite end; its signal provides a continuous output proportional to the integrated light scattering. A reference photodiode views the light source, continuously monitors the light output, and maintains a constant light intensity by means of an electronic regulator. Filters in front of the photomultiplier and photodiode closely approximate the spectral response of the human eye.

The photomultiplier tube operates in a photon-counting mode that provides a sequence of output pulses proportional to the amount of scattered light. These pulses are processed through the necessary electronic circuitry to provide an analog output. The output then drives a display meter and is available for recording.

By switch selection, the sample chamber can be filled with clean air, thus providing a simple "clean air check." This can be done manually or automatically with the addition of an appropriate timer. The nephelometer can be calibrated with particle-free gases such as Freon 12 or Freon 22. These gases are inexpensive and have known scattering coefficients.

NEPHELOMETER LIMITATIONS

The nephelometer measures light scattering in the atmosphere at a single geographical point; its applications are limited to cases where there is spatial uniformity of atmospheric properties. Errors may be introduced by differences in relative humidity inside the instrument relative to ambient conditions. The instrument can have two types of error if atmospheric optical properties are controlled by particles larger than 3 microns, such as in fog or dust

* The mention of commercial products in connection with materials reported herein is not to be construed as either an actual or implied endorsement of such products.

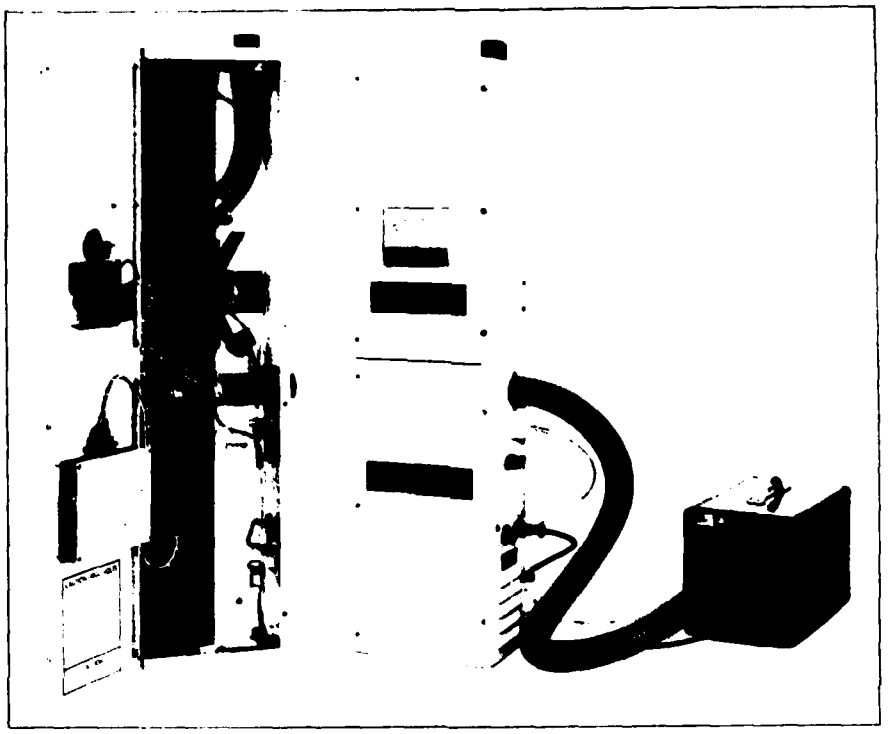

SPECIFICATIONS

PERFORMANCE

SCATTERING COEFFICIENT		0–2.5 X 10^{-4} m^{-1}
LOCAL VISUAL DISTANCE		16 TO 300 KILOMETERS
EFFECTIVE SCATTERING WAVELENGTH		CENTERED AT APPROXIMATELY 530 NANOMETERS
OUTPUT	VOLTAGE	0 TO 5 VDC
	IMPEDENCE	<100 OHMS
AIR SAMPLE RATE		MINIMUM OF 100 LITERS PER MINUTE

ENVIRONMENT

TEMPERATURE	-10^{o}C TO $+50^{o}$C
RELATIVE HUMIDITY	0 TO 95%
ALTITUDE	SEA LEVEL TO 5,400 METERS

POWER

105 TO 125 VAC, 60 Hz	70 WATTS MAXIMUM

DIMENSIONS

OPTICAL ASSEMBLY	
HEIGHT	100 cm
WIDTH	25.5 cm
DEPTH	16 cm

WEIGHT

OPTICAL ASSEMBLY	12.4 kg

FIGURE 2. Integrating Nephelometer Used by NWC (MRI Model 1560).

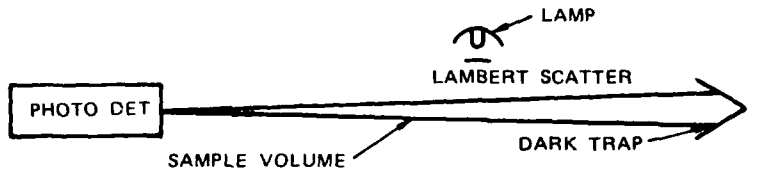

OPTICAL GEOMETRY OF INTEGRATING NEPHELOMETER

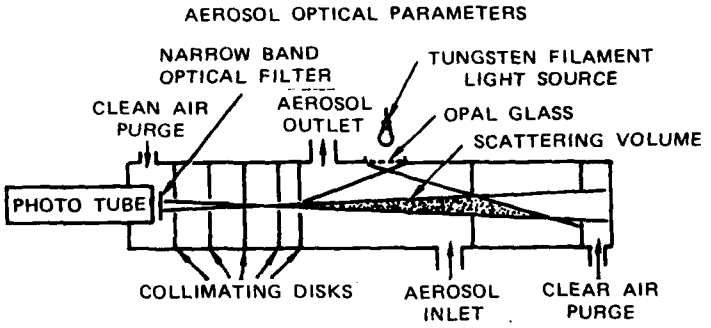

FIGURE 3. Diagram of Integrating Nephelometer.

storms: (1) coarse particles will be excluded from the sample chamber by impaction on the sampling ductwork, and (2) the angular integration suffers from truncation at low scattering angles and in fog will underestimate the actual scatter coefficient by up to a factor of 2. Fortunately, most man-made haze particles are less than 3 microns in diameter, so these errors have not proven to be important.[7]

Finally, the nephelometer measures only the amount of light that has been scattered by particles and gases in the atmosphere; it does not take into account the light that has been absorbed by the particles and gases. Again, fortunately, in remote areas such as China Lake it appears that the absorption component is much smaller than the scattering component, so the error is not critical to this particular application. However, any absorption that does occur in the sample chamber will bias the results. Specifically, if scattered light is subsequently absorbed, then the determination of scattering coefficient will be low.

A more complete discussion of light scattering and absorption can be found in Appendix A.

[7] J. R. Ouimette, R. C. Flagan, and A. R. Kelso. "Chemical Special Contribution to Light Scattering by Aerosols at a Remote Site," presented at the 2nd Chemical Congress of North American Continent, Las Vegas, Nev., 27-29 August 1980. Paper UNCLASSIFIED.

METEOROLOGY AND VISIBILITY

In studying the visibility impairment problem one must consider the frequency of occurrence of meteorological conditions that could result in increased values of the extinction coefficient, especially particle scattering. The concentration of suspended aerosols in the China Lake (Indian Wells Valley) area is the result of a variety of meteorological conditions. Basically, it appears that visibility at China Lake is affected by long range transport of aerosols; wind blown dust; topographically trapped smoke plumes, vehicle exhaust, and road dust; and fog.

LONG RANGE TRANSPORT OF AEROSOLS FROM URBAN AREAS AND SAN JOAQUIN VALLEY

Urban pollutants transported by the winds aloft are the most common visibility restriction problem in the China Lake area. Aerosol matter of both natural and anthropogenic origin, primarily the latter, is routinely advected into the Indian Wells Valley from sources outside the local area.[7-8] This transported aerosol is a fairly homogeneous air mass that can arrive from a variety of sources and a variety of routes. These particle masses can at times be several thousand feet thick and negotiate barriers such as the Sierra Nevada mountains. Transported urban haze is a daily phenomenon occurring throughout most of the spring, summer, and fall months. Sulfur hexafluoride (SF_6) tracer experiments have demonstrated transport of pollutants from Bakersfield to China Lake.[9] Numerous observations of polluted air moving east through Walker and Tehachapi Passes, and north through the southern (Red Rock Canyon) passes (see Figure 4) indicate that Indian Wells Valley is essentially at the mercy of the upper winds and air mass history as to what the relative concentration of aerosols might be on any given day. Since the prevailing airflow is from the south and west through Walker Pass and Tehachapi Pass, the encroaching polluted air mass can be observed routinely coming from that direction and typically reaches the Indian Wells Valley in the late afternoon.[8] Large-scale urban plumes can have residence times of up to a week or more and can transport urban aerosols distances exceeding 1000 miles.

WIND BLOWN DUST GENERATED LOCALLY OR FROM OWENS LAKE

Strong northerly winds (which do not occur frequently in the Valley) may cause a rapid decrease in visibility, especially over the northern and western parts of the Valley. This sharp visibility decrease is the observed result of alkali dust from Owens Lake and beyond, blowing through the mountain gaps northwest and north of Indian Wells Valley (see Figure 4).[10] The

[8] J. R. Ouimette. "Aerosol Chemical Species Contributions to the Extinction Coefficient," Ph.D. dissertation, California Institute of Technology, Pasadena, Calif., July 1980.

[9] Danny D. Reible, James R. Ouimette, and Frederick H. Shair. "Visibility Degradation Associated with Atmospheric Transport into the California Mojave Desert," accepted by *Atmospheric Environment*.

[10] P. St. Amand, L. Mathews, and R. Reinking. "Dust Storms Due to Desiccation of Owens Lake," presented at the International Conference on Environmental Sensing and Assessment, Las Vegas, Nev., 14-19 September 1975. Paper UNCLASSIFIED.

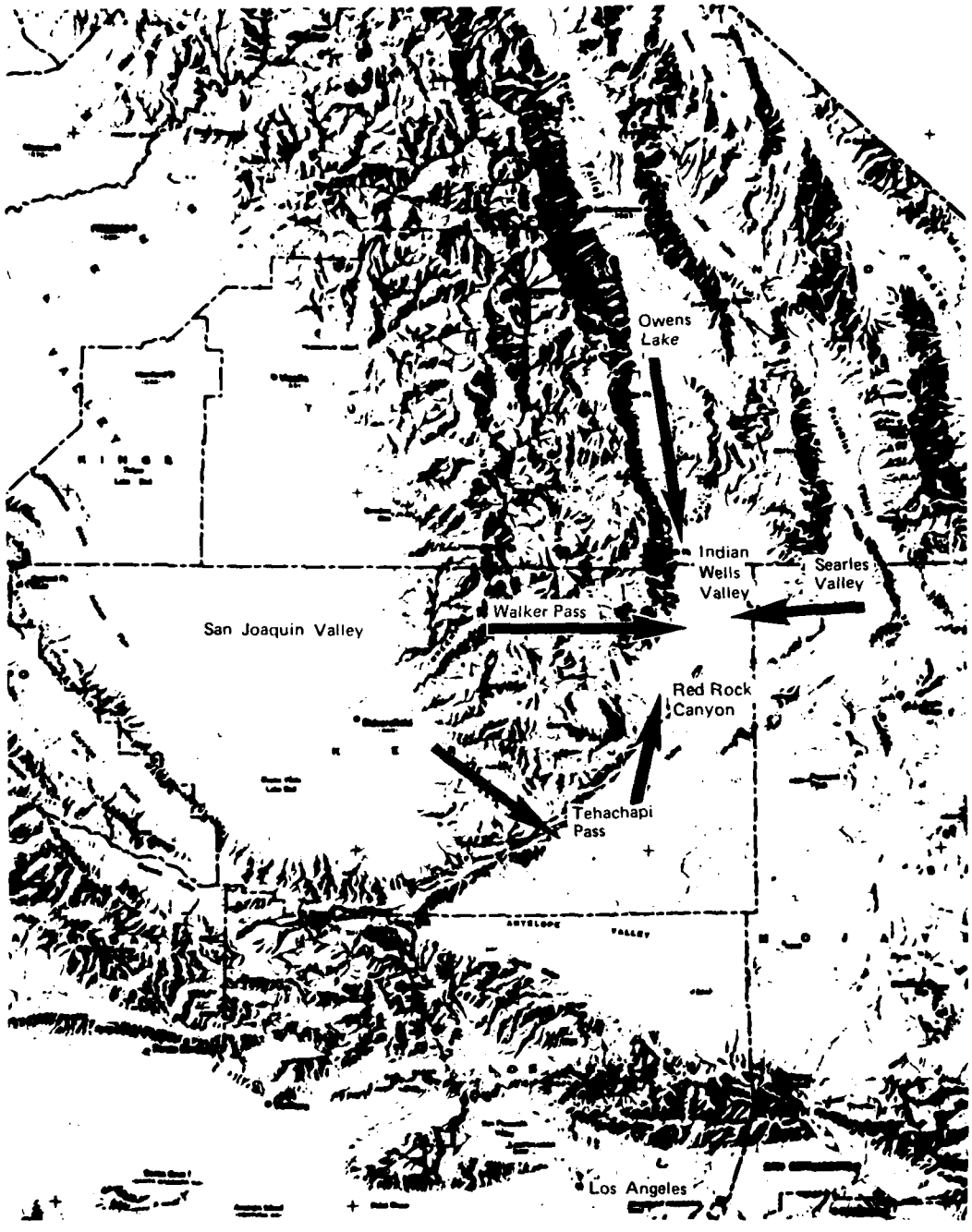

FIGURE 4. Map of the Indian Wells Valley and Surrounding Area Depicting Transport of Dust and Pollutants by Winds. Winds aloft transport pollutants east through the Walker and Tehachapi Passes, and north through the southern passes (Red Rock Canyon). Wind blown dust is transported south from Owens Lake through the Little Lake gap, and industrial plumes are transported east from Searles Valley.

year-to-year occurrence of these winds has been erratic, estimated at 20 to 25 days per year and mostly in the months of November through March.

Wind-blown sand is usually caused by a southerly or northerly surface wind component in excess of 25 to 30 mph. When a moderate to severe dust storm occurs, visibilities are reduced to as low as 1/2 to 1 1/2 miles for 1 to 2 hours.[10] Local dust storms occur approximately 15 days per year, closing NWC's Armitage Airfield on the average of 3 to 4 days per year.*

TOPOGRAPHICALLY TRAPPED SMOKE PLUMES, VEHICLE EXHAUST, AND ROAD DUST

Stagnant air masses and temperature inversions occurring in the local valleys (Indian Wells Valley and Searles Valley) during the fall, winter, and spring months restrict vertical mixing and at times greatly reduce visibility at the lower altitudes. Industrial plumes such as those produced by the Kerr-McGee Chemical Corporation can greatly affect visibility and are caused by primary and secondary particles and possibly nitrogen dioxide (NO_2). The plumes from the Kerr-McGee plants at Trona, West End, and Argus (in Searles Valley) are the largest stationary sources of pollution in the Upper Mojave Desert.** Hydrogen sulfide (a potential source of scattering particulate) (H_2S) concentrations measured near the Trona facility during an 18-month period, averaged several hundred parts per billion with frequent peaks of 500 parts per billion (ppb). Frequent visual observations indicate that the Searles Valley plume enters the Indian Wells Valley from a variety of unnamed passes. The wind rose data of Figure 5 show that the wind blows from the direction of the Searles Valley 10-18% of the time, suggesting a potential encroachment of the Searles Valley plume into the Indian Wells Valley 10-18% of the time depending on the local easterly winds, seasonal considerations, and other meteorological factors.

Local automobile traffic accounts for one half of the pollutants generated in Indian Wells Valley. Traffic on Highways 14 and 395 are significant contributors relative to other automobile sources. Other emission sources are fugitive dust from dirt road traffic, construction activities, and materials handling. Activities at NWC contribute to the aerosol budget by aircraft exhaust, boiler plant emissions, and assorted cook-off plumes.[11] Also, during the winter months smoke from wood burning fireplaces is trapped below the strong inversion, adding to the absorption coefficient as well as the scattering coefficient.

*Personal communication with J. Gibson NWC meteorologist, 1980.

**Emission rate data received from San Bernardino County Desert Air Pollution Control District, San Bernardino, California. Data show emission rates for 1978.

[11] Naval Weapons Center. *Survey and Evaluation of the Environmental Impact of Naval Weapons Center Activities*, by James R. Ouimette. China Lake, Calif., NWC, June 1974. (NWC TM 2426, publication UNCLASSIFIED.)

FOG

Fog is a minor factor in limiting visibility in Indian Wells Valley. Foggy conditions may occur after winter rains or snow. Fog depth and duration is dependent on temperature and moisture, and is usually on the order of 1 or 2 days after a rain or snow, burning off in the afternoon. The frequency of fog is estimated at 5 to 10 mornings per year, occurring between November and March.

The above four phenomena are the result of complicated effects of (1) topographical and geographical factors, (2) surface and upper winds, and (3) diurnal and seasonal meteorology. Each of these factors will be addressed in the following section.

LOCAL METEOROLOGY

Overview

Desert regions tend to be windy. Surface winds in the Indian Wells Valley are predominantly from the southwest or west-southwest (see Figure 5), with a tendency toward the more westerly direction during the winter months.[12] The predominant winds and air mass history determine the externally generated aerosol load affecting the Valley. Two main factors affect the local wind circulation: (1) The mountains surrounding the Indian Wells Valley and (2) the airflow into the Valley at low levels through three main passes—Walker and Red Rock Passes to the southwest, and Little Lake Gap to the north-northwest.

Because of the topography of the Valley, the surface winds do not necessarily follow the pattern of the winds aloft, as might be expected, but are often forced around the mountains and accelerated through the passes (see Figure 4). This creates jet-like force winds to one sector of the valley and light or variable winds to other sectors. Thus, with moderate westerly winds aloft, there may be strong southwest surface winds over some sectors. At other times, strong northwest winds aloft may never reach the surface, or they may affect only the western side of the valley.[12]

The highest wind velocities, with associated dust and sandstorms, are reached during the late winter and spring months, with the maximum number of hours of winds exceeding 30 mph coming between February and June. During the summer months the tendency is toward fewer hours of excessive winds and more hours of moderate velocity winds (20 to 30 mph). During this period the maximum wind speed exceeds 20 mph on 20 to 30 days out of the month, with little or no dust, however. This maximum occurs late in the afternoon. Strong surface winds at night are rare but occur with the passage of fronts, thunderstorms, or the presence of a deep low pressure system in the immediate vicinity. When certain pressure conditions exist, strong

[12] Naval Ordnance Test Station. *A Climatological Summary of Surface and Upper Air Weather at NOTS*, by P. H. Miller. China Lake, Calif., NOTS, December 1962. (NOTS TP 3003, NAVWEPS Report 7960, publication UNCLASSIFIED.)

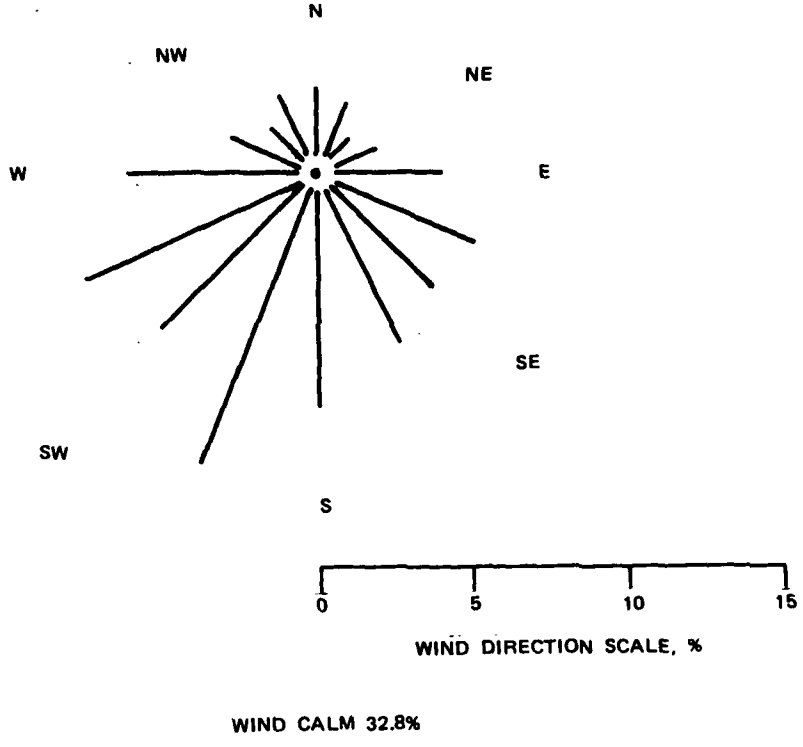

FIGURE 5. Surface Wind Directional Frequency Based on Data from January 1973 Through January 1977.

winds from the southwest and northerly directions occur. When the airflow aloft is strong from the west or north, the winds on the lee side of the mountains (the side away from the direction from which the wind blows) may be very erratic.[12]

Effects of Daily Weather Variations

Due to its interior location, Indian Wells Valley has relatively severe seasonal temperatures and a consequent wide annual temperature range. Diurnal variations of 40°F are typical. During the summer months the maximum temperature occurs around 4 p.m. each day and the minimum between 4 and 5 a.m. PST. In the winter the maximum occurs between 1 and 2 p.m. and the minimum between 6 and 7 a.m. PST.[12]

Surface Winds. During the night and early morning hours light winds generally prevail, and moderate-to-strong winds frequently rise during the afternoon. These relatively high afternoon winds are caused by high diurnal temperature variations and resulting pressure gradient differentials. The high degree of surface heating in the afternoon can cause air currents and possibly dust devils.[12]

Temperature Inversions. During a temperature inversion there is a decrease in potential temperature with height. Temperature inversions can dramatically affect visibility (especially

during the winter) and can prevent the mixing of materials in the atmosphere. Although the lack of wind on calm winter days can effectively prevent long range transport of pollutants into the Valley, depending on air mass history, locally emitted pollutants are trapped in the stagnant air mass and do not disperse until the inversion lifts.

The inversion layer condition (generally a winter condition) occurs when the southwestern United States is dominated by a Great Basin high pressure system, which may persist for 3 to 5 days. This high pressure system is accompanied by clear, subsiding, dry air aloft and nearly calm winds at the surface during the night.[12] The local winds may have an easterly component and potentially bring the Searles Valley plume into the Indian Wells Valley. These conditions are favorable for considerable radiational surface cooling at night, resulting in the formation of a sharp temperature inversion from the ground upward. The stratification in the lower layers is very stable, and therefore unfavorable to mixing processes that would distribute locally generated pollution throughout a deeper layer.

The depth of the surface-based inversion depends on the absence of wind and convective motion. Very light winds or calm conditions are necessary to produce an intense inversion; strong winds near the surface, which tend to mix the surface cold air with the warmer air above, destroy the inversion. In the majority of cases light winds prevail at night, producing an intense inversion at sunrise.[12] Winter morning mixing heights of less than 200 feet are quite common.

Whether the inversion will dissipate completely depends upon the temperature rise during the day. If the inversion is completely dissipated and if sufficient moisture is present in the atmosphere, continued surface heating may cause convective currents to rise, producing gusty winds and cumulus clouds.[12]

SUMMARY

It is recognized that there are characteristic properties of different air masses in the large-scale weather patterns. These different types of air masses can be identified, and they illustrate the dependence of aerosol properties and concentrations on air mass history. The combination of regional-scale weather patterns and local and regional topography combine to produce conditions that have a fundamental relationship to local visibility—especially as the extinction coefficient is dominated by aerosol contributions.

On a seasonal basis, in winter the high pressure systems dominate with traveling storms and recurrent trough passage. The occurrence of a very clean, clear, cool, subsiding air mass associated with the high pressure system leads to a stable atmospheric condition. The principal air movements are convective motion accompanying daytime surface heating and downslope motion accompanying intense nighttime radiation cooling. Subsequent entrapment of local pollutants within the resultant steep radiation-inversion is the major mechanism that increases the local aerosol load at surface level. Wintertime traveling storms generally bring clean, clear, cold, air and wind that may stir up quite a bit of dust, with obvious results. Precipitation is a predictable and short term detriment to good visibility. Fog forming from the resultant ground moisture is likewise predictable, infrequent, and of short duration.

Summertime brings air masses from the west, south, and east in response to the thermal low generally existing across the southwestern United States.[12] Air masses coming from the west will generally have passed through the San Francisco Bay area and San Joaquin Valley en route and will be heavily polluted as a result. If southerly flow dominates, air from the South Coast Basin including Los Angeles, Antelope Valley, and eastward may arrive. This air, too, contains a considerable mass of aerosols. With southeasterly flow, air may arrive from the Gulf of Mexico. Sometimes sufficient thunderstorm activity will have "cleaned" the air so that only a moderately increased aerosol burden remains.

Both aerosol concentration and size distribution affect visibility. Determining the extinction coefficient most commonly associated with these different air masses (each with different histories) is a difficult and necessary task if one is to understand "visibility" in the area.

SUMMARY OF NEPHELOMETRY DATA

DESCRIPTION OF DATA BASE

The visibility data presented in this report were derived from the continuous collection of particle scattering values through atmospheric nephelometry. Both daytime and nighttime measurements are included, and hourly averages of the particle scattering values have been summarized for the period September 1975 through September 1980. Data quality problems due to instrument modifications occurred throughout the 5-year period. The problems were minimized by close scrutiny of the data at many phases; parameters such as wind speed, wind direction, temperature, dewpoint, precipitation, and ozone content were correlated in analyzing questionable data. The number of hourly averages used as data points for computing all statistics is shown in the data points summary. A quick glance at the summary for any given year indicates how much data are missing or have been excluded (1 year contains 8,760 hours).

Data points summary, hourly averages

Sep 1975	2,146	
1976	6,238	
1977	6,775	
1978	7,915	
1979	8,231	
Sep 1980	5,989	
Total	37,294	85%

The data are presented as particle scattering values rather than visual range unless otherwise stated. All particle scattering values are in units of inverse meters ($X10^{-6}m^{-1}$). The visual range scale shown on the right side of the graphs and figures was calculated using data and formulas that are presented in Appendix A.

SEASONAL TRENDS

Figure 6 shows that the monthly average data vary substantially on a monthly basis, but by combining data for like months (Figure 7), seasonal trends can readily be seen. Table 1 summarizes the data displayed in Figures 6 and 7.

Figures 8 and 9 display a pronounced seasonal variation, and these patterns are usually consistent from year to year. Visibility is lowest during the summer (May to August), when the calculated median visual range is 68 kilometers (42 miles), and highest during the winter months (November to February), when the median visual range is 123 kilometers (76 miles).

Historically, May is the worst month for visibility, with a mean b_{sp} value of 40.98 $\times$ $10^{-6}m^{-1}$; June is a very close second with a mean of 40.64 $\times$ $10^{-6}m^{-1}$. August is third and July fourth, with means of 38.74 $\times$ $10^{-6}m^{-1}$ and 36.04 $\times$ $10^{-6}m^{-1}$, respectively. The combined mean for May through August is 39.10 $\times$ $10^{-6}m^{-1}$, while the combined mean for the remaining eight months is 25.76 $\times$ $10^{-6}m^{-1}$. The best month for visibility is January with a mean of 19.55 $\times$ $10^{-6}m^{-1}$. The mean b_{sp} value for the entire data base is 30.47 $\times$ $10^{-6}m^{-1}$, with a median of 25.52 $\times$ $10^{-6}m^{-1}$. Figure 6 shows the monthly b_{sp} values for the entire data base.

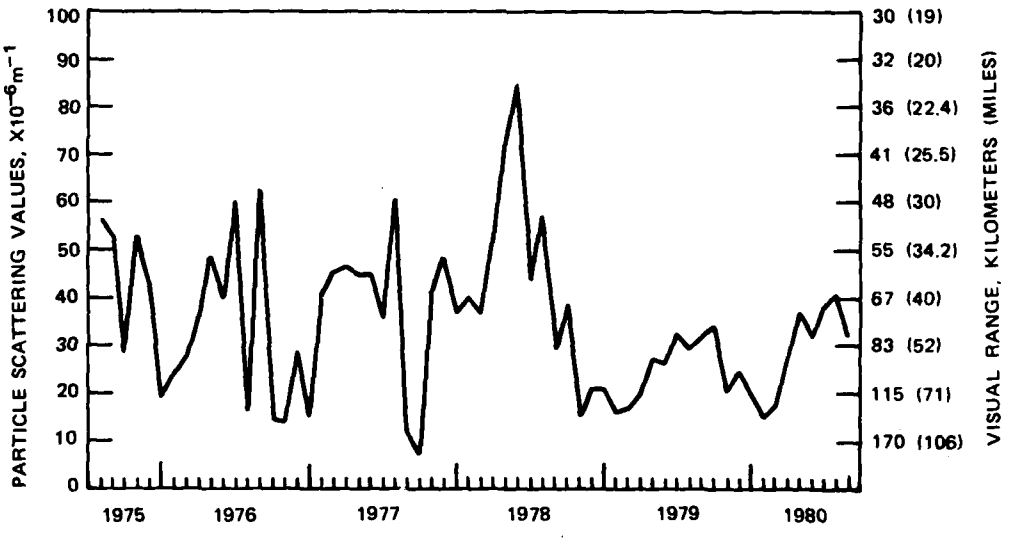

FIGURE 6. Monthly Particle Scattering Averages for 1975 through 1980.

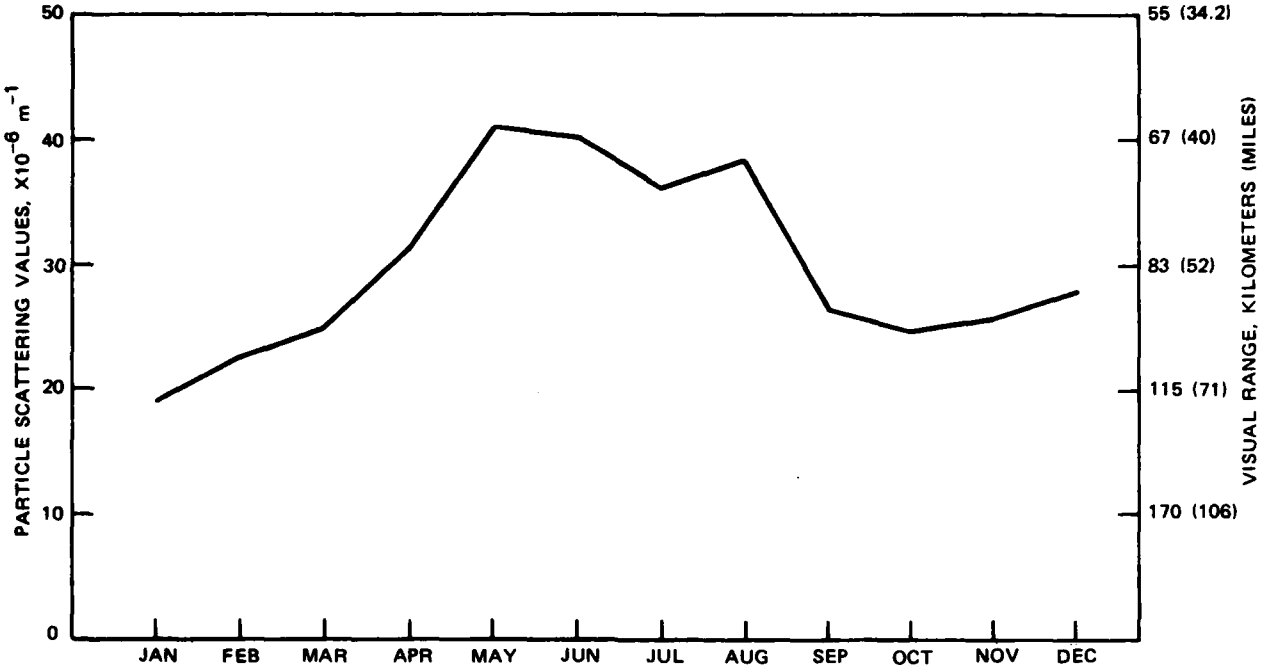

FIGURE 7. Monthly Particle Scattering Averages for 1975 through 1980.

TABLE 1. Summary of Monthly Particle Scattering Averages for 1975-1980.

Month	Average particle scattering values, X10^{-6}m^{-1}						
	1975	1976	1977	1978	1979	1980	1975-1980
Jan	...	16.57	13.13	32.24	18.49	17.47	19.55
Feb	...	20.98	35.79	35.10	14.09	13.09	23.78
Mar	...	24.25	39.66	32.30	15.16	15.63	24.96
Apr	...	31.75	40.86	45.90	17.94	23.91	31.97
May	...	42.86	39.23	64.61	24.08	32.72	40.98
Jun	...	34.54	39.38	74.71	23.07	27.51	40.64
Jul	...	52.93	30.93	38.17	28.77	33.32	36.05
Aug	49.59	14.11	53.55	50.27	25.81	35.73	38.74
Sep	46.13	55.12	10.40	25.43	28.16	28.11	26.88
Oct	25.10	12.88	6.23	34.28	30.16	...	25.32
Nov	46.47	12.39	36.01	13.01	17.80	...	25.90
Dec	36.49	25.39	42.59	18.50	21.55	...	27.73
Yearly averages	37.95	29.79	33.55	39.01	22.17	25.15	30.47

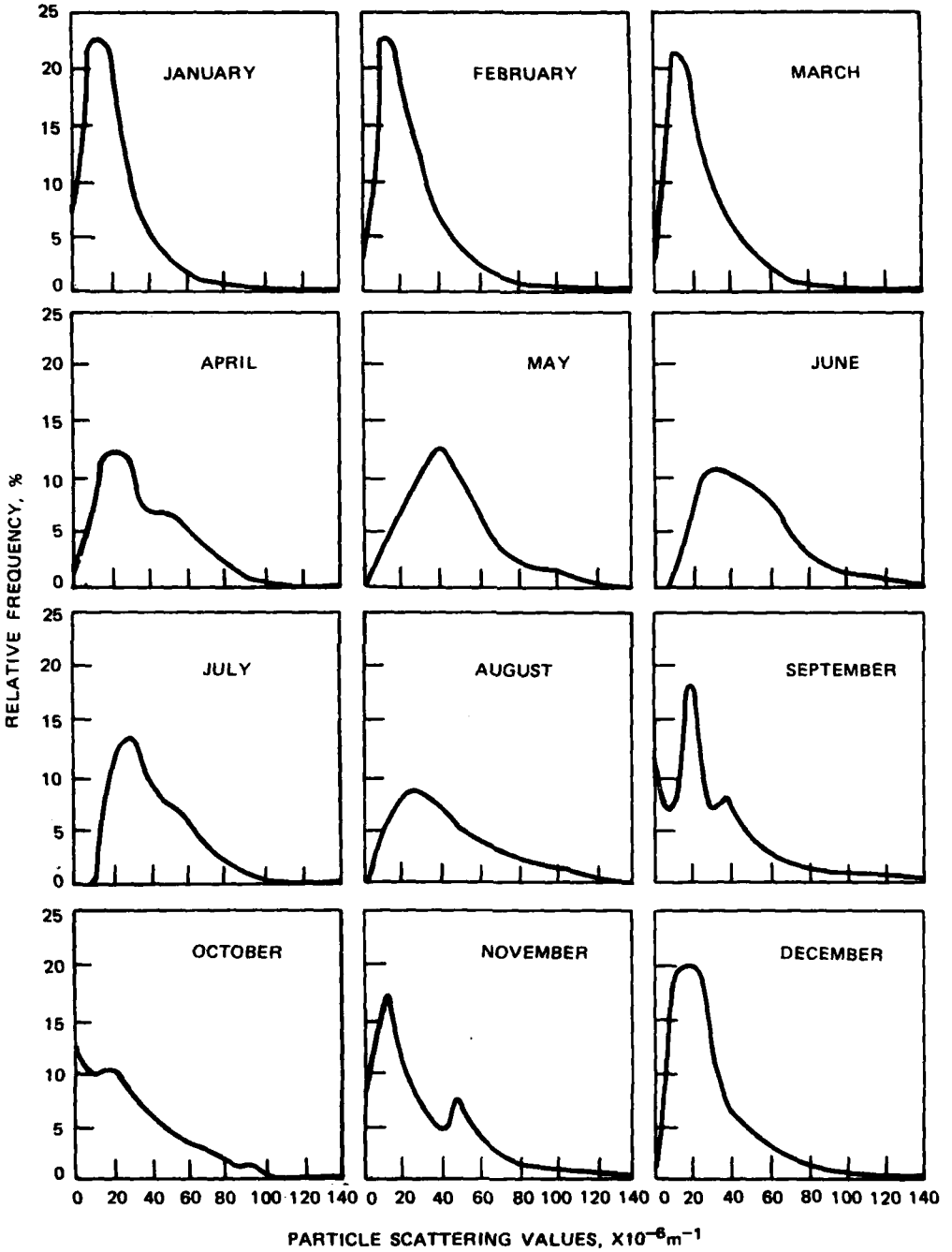

FIGURE 8. Particle Scattering Frequency Distribution by Month for the 5-Year Data Base (1975-1980). Each plot shows the average particle scattering for that month during the 5-year period.

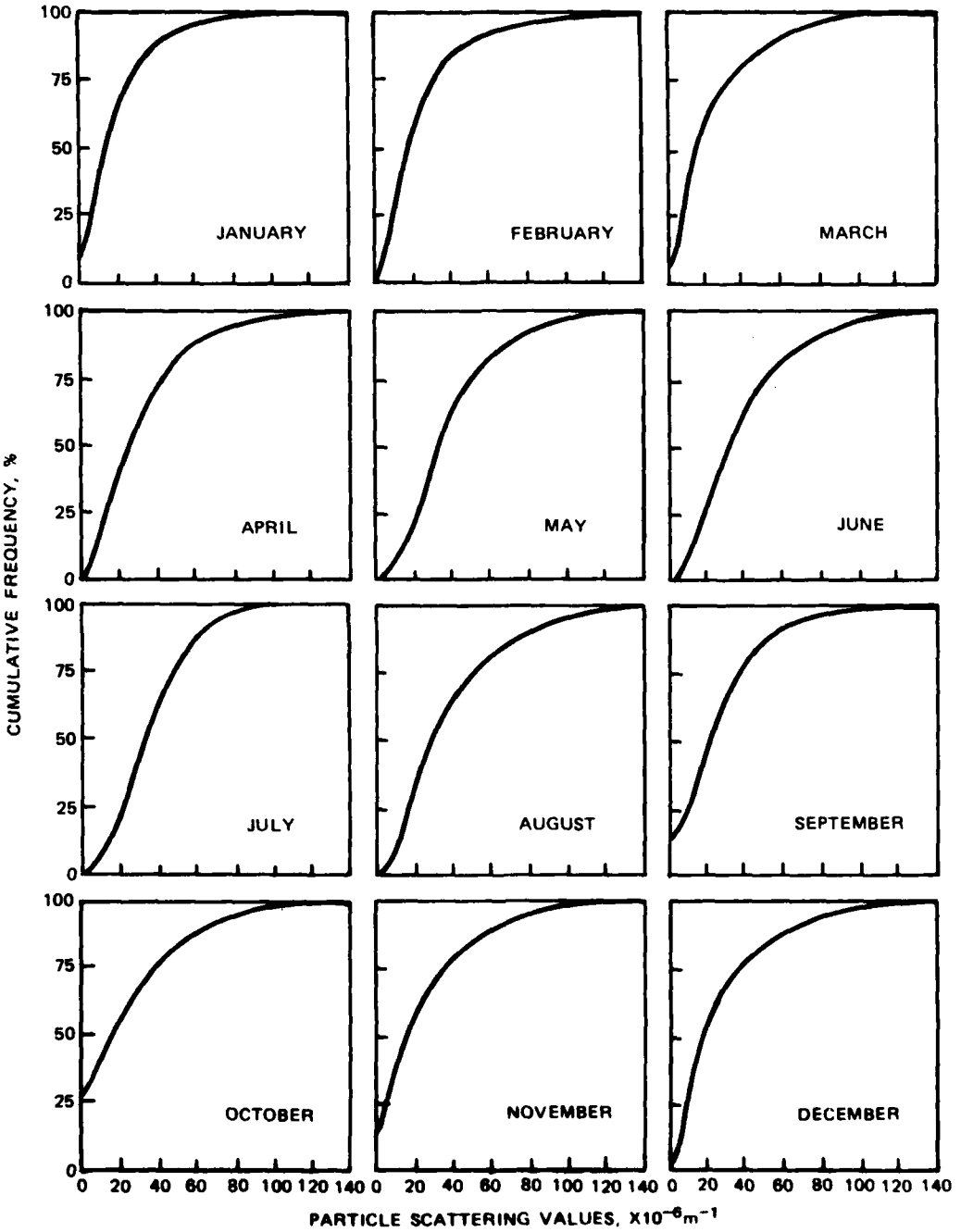

FIGURE 9. Cumulative Particle Scattering Frequency Distribution by Month for the 5-Year Data Base (1975-1980). Each plot shows the cumulative particle scattering for that month during the 5-year period.

Table 2 presents combined hourly b_{sp} data for like months for the entire data base. These same data are portrayed on a monthly basis in Figure 10. A few rather general observations are germane at this point. With respect to these hourly mean values, January is the lowest month, while May is the highest. March is the flattest, or most uniform, while June is the most highly variable, or bumpiest. Fundamental similarities are seen in data for November, December, and January—the winter months. Similarly, June, July, and August are clearly similar. Particularly well matched are the equinox months of March and September. February and October are generally alike. April and May exhibited similar time histories of b_{sp}—except for May's higher baseline.

TABLE 2. Summary of Hourly Particle Scattering Values Averaged by Month for the Years 1975-1980.

Hour	Average particle scattering values, $X10^{-6}m^{-1}$											
	Jan	Feb	Mar	Apr	May	Jun	Jul	Aug	Sep	Oct	Nov	Dec
0	23.45	26.23	28.92	38.92	48.81	51.39	42.85	45.20	30.24	27.83	28.95	33.34
1	22.09	26.16	24.80	33.55	48.77	51.53	43.61	45.68	32.19	27.10	30.16	31.69
2	21.84	23.53	24.86	34.78	45.25	46.31	42.50	49.01	31.52	26.86	29.59	29.02
3	20.11	23.26	26.88	34.37	44.96	49.07	42.35	46.22	33.20	26.46	27.38	24.44
4	19.18	23.57	26.54	34.37	45.32	49.37	42.17	46.40	32.08	26.50	27.29	23.52
5	18.30	22.36	27.98	34.91	46.37	48.77	42.80	45.96	30.46	25.16	25.88	23.39
6	17.59	23.01	29.20	33.85	46.46	49.30	42.89	47.57	31.08	26.72	25.14	22.73
7	18.90	23.02	28.94	34.11	44.22	48.70	43.27	47.90	32.53	26.85	25.01	23.17
8	19.73	24.38	29.51	36.14	43.11	45.02	42.17	46.41	31.42	29.28	25.69	23.90
9	20.12	25.78	29.77	34.51	41.02	40.12	39.22	42.52	29.37	29.82	25.67	24.97
10	18.31	26.32	26.18	30.34	39.78	35.15	35.53	38.54	26.70	27.02	23.50	24.54
11	18.76	23.07	31.35	26.86	37.41	32.38	31.14	34.43	22.89	24.03	21.91	22.88
12	17.20	21.50	20.34	25.05	36.00	29.46	27.52	27.76	20.50	20.72	19.98	21.74
13	14.34	19.29	18.94	25.57	34.86	27.28	24.80	25.00	19.35	20.40	17.95	18.80
14	12.58	18.66	20.05	25.02	33.07	26.84	23.34	24.32	18.07	18.08	17.08	18.70
15	11.84	18.30	18.75	25.51	33.11	27.29	23.67	23.62	17.49	18.50	18.42	17.67
16	12.39	18.97	18.90	26.63	36.61	29.28	25.64	25.94	18.53	18.69	19.91	19.41
17	14.10	19.71	21.93	26.92	36.70	32.02	28.15	30.17	20.06	20.61	22.23	22.93
18	17.81	22.15	19.98	29.48	35.22	36.41	31.35	32.60	22.49	23.26	23.05	28.20
19	22.74	25.57	24.70	33.90	37.96	40.72	34.46	36.93	25.77	26.10	31.02	42.65
20	26.54	29.61	27.37	35.65	41.04	43.48	37.53	40.86	28.66	27.73	36.36	45.34
21	28.05	30.11	27.29	35.57	43.00	46.21	39.74	42.19	30.47	28.51	34.94	44.63
22	27.68	29.77	28.80	36.34	43.40	46.81	40.57	43.14	30.67	30.29	32.88	41.47
23	25.40	26.88	28.56	36.35	43.99	46.30	40.64	42.51	30.18	31.41	31.00	35.93

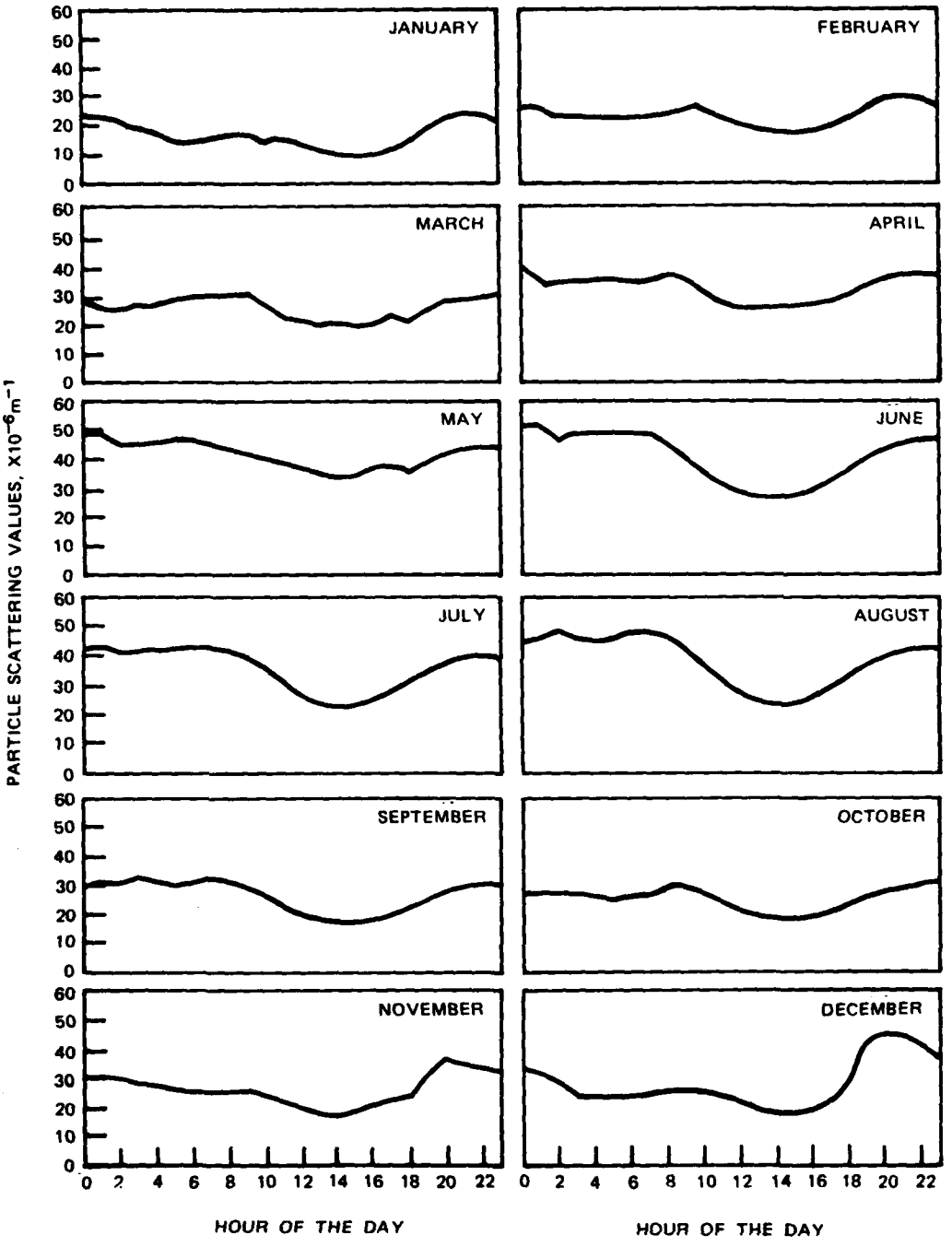

FIGURE 10. Diurnal Trends. All data have been averaged such that each plot depicts a "typical" day for that month. Note that greatest visibility generally occurs at hour 14 (2 p.m. PST).

DIURNAL TRENDS

Diurnal patterns appear when the data are combined on an hourly basis for all months (Figure 10). The data show a pattern of increasing visibility during the course of the daylight hours with the best visibility typically in the early afternoon (Figures 10 and 11). Normally the time of maximum visibility is 2 p.m. PST. The time of minimum visibility is more variable (usually occurring at night).

The diurnal variation in light scattering due to particles in the atmosphere (b_{sp}) is coupled to the diurnal cycle of afternoon winds and nighttime inversions. Frequently polluted air from urban sources is transported by winds in the early evening and trapped by a stable inversion through the night, causing elevated values of b_{sp}. The inversion lifts the next morning, reducing the b_{sp} by mixing with cleaner air aloft. A minimum in b_{sp} then occurs in the midafternoon before the cycle repeats in the evening.[8]

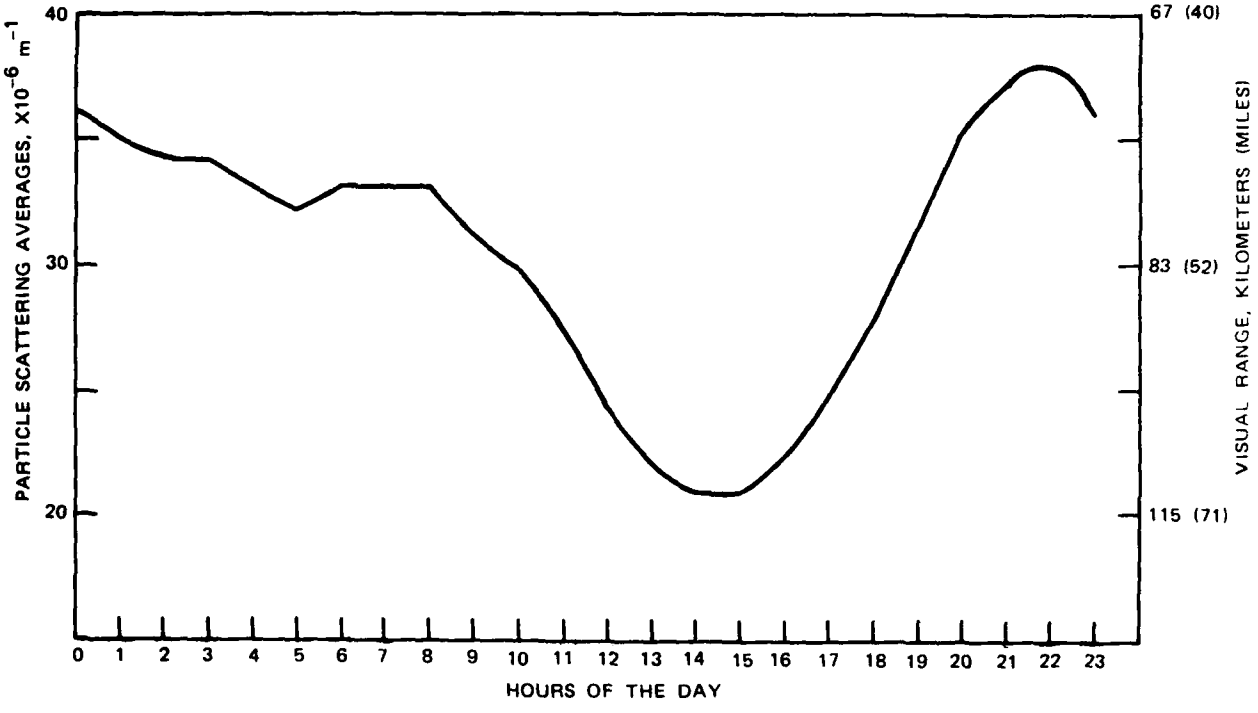

FIGURE 11. Diurnal Trend. All data for the 5-year collection period have been averaged to show this daily trend.

CUMULATIVE FREQUENCY DISTRIBUTION

A data base of this size is more appropriately summarized by cumulative frequency and frequency distribution (Figures 12 and 13). The cumulative frequency distributions can easily display best case (10%) and worst case (90%) as well as median (50%) visibility.

Most interesting are Figures 14 and 15. Note the summary of the monthly cumulative distribution trends of 90% (worst case), 50% (median), and 10% (best case) data (Figure 15). The median visibility for the entire data base is 94 kilometers (58 miles), the mean visibility is

approximately 82 kilometers (51 miles), and the best 10th percentile visiblity ranges from 296 to 123 kilometers (194 to 76 miles) with an average of 202 kilometers (125 miles). The worst case (90th percentile) visibility ranges from 47 to 33 kilometers (29 to 20 miles) with an average

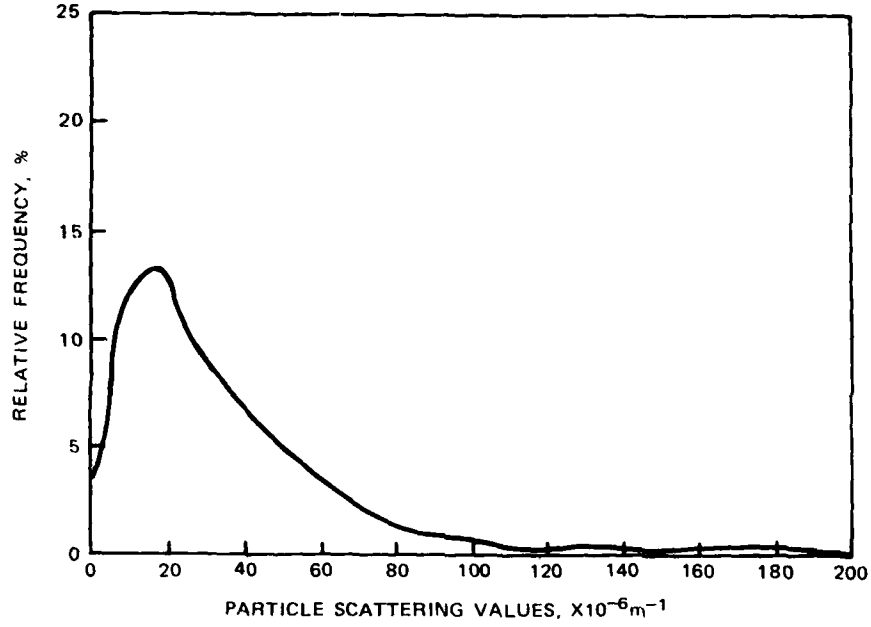

FIGURE 12. Particle Scattering Frequency Distribution for the 5-Year Data Base (1975-1980).

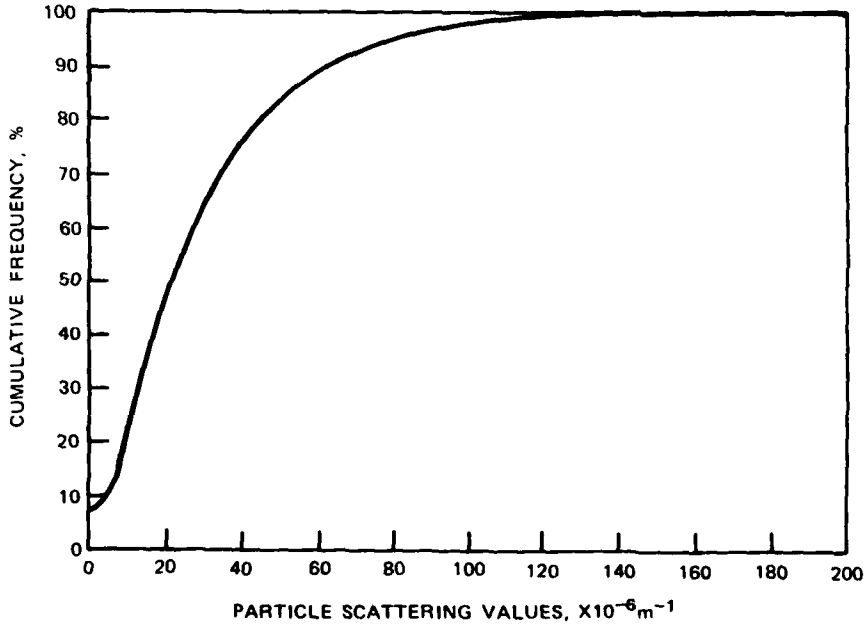

FIGURE 13. Cumulative Particle Scattering Frequency Distribution for the 5-year Period (1975-1980).

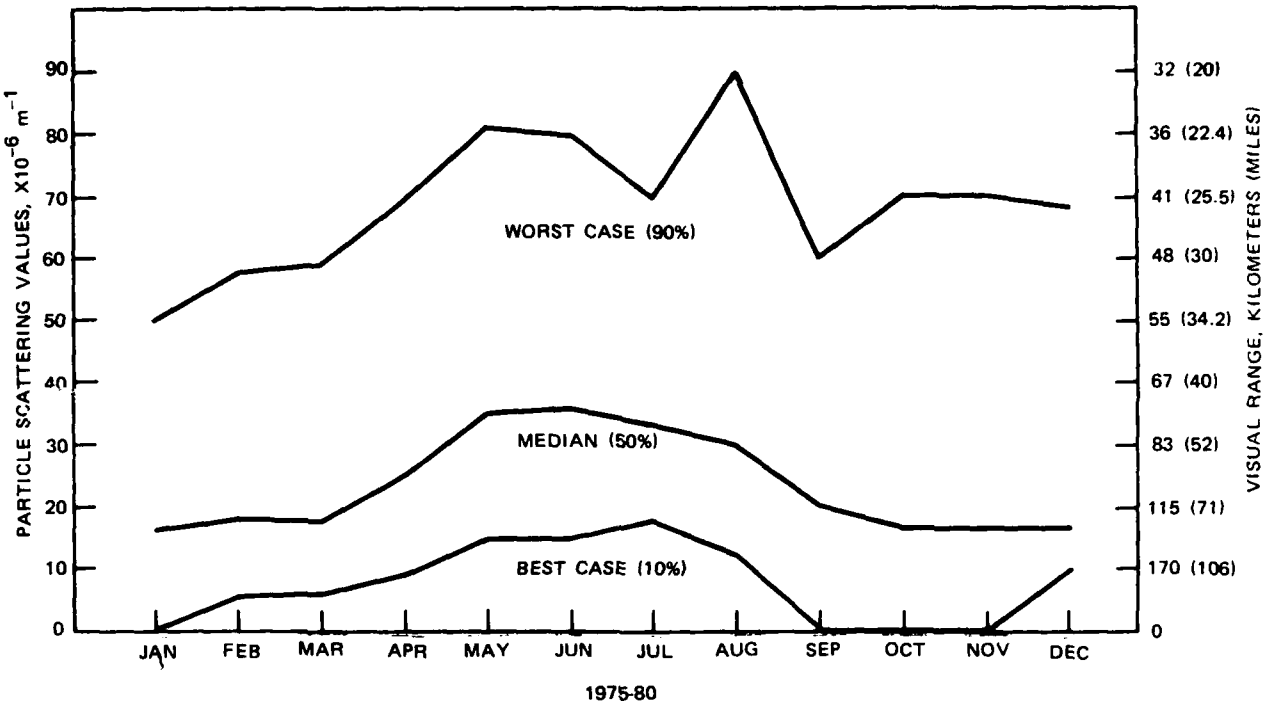

FIGURE 14. Summary of Monthly Cumulative Distribution Trends.

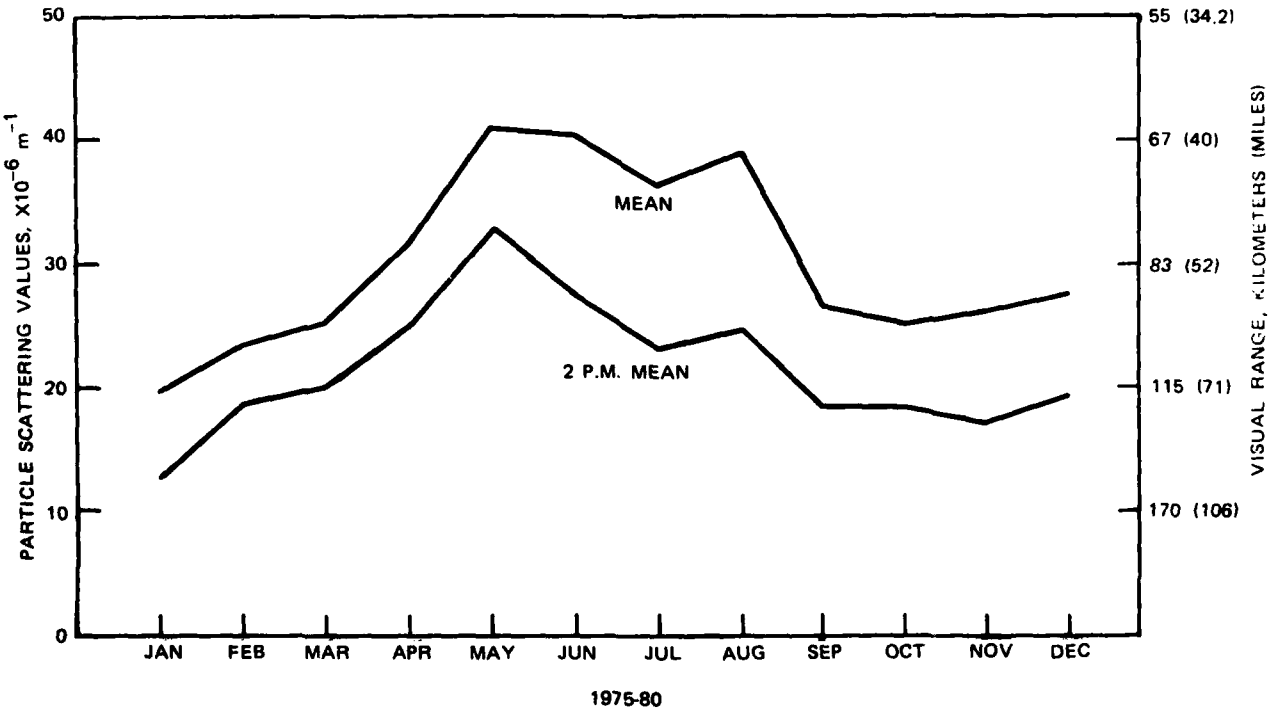

FIGURE 15. Average Monthly Mean Visibilities Compared to Average 2 p.m. Visibilities.

of 41 kilometers (26 miles). Note the mean 2 p.m. PST values in Figure 15. The early afternoon visibilities are much greater than the normal median value, and this value more closely reflects perceptions of daytime visibilities at China Lake. The mean 2 p.m. PST visual range is 107 kilometers (66 miles).

METEOROLOGICAL EFFECTS

The best visibilities are associated with upper air transport from areas of low population density (in our case the north). However, air transport from the north has a high potential for windblown dust.[12] Owens Lake dust can be a major source of visibility degradation. Long range transport of fine aerosols is the dominant contributor to visibility degradation in the Indian Wells Valley and the desert southwest on typical days. Blowing dust and sand is the dominant factor on worst case days.

The persistence of daytime moderate to low wind speeds is more than adequate to transport urban haze into the valley[9] where it can be trapped by the local topography at night. (The only dilution factor is the vertical mixing depth, which increases with ground warming.) The next day the winds may not be strong enough for this air mass to move out of the valley. During periods of higher than average winds heavily polluted air that is advected into the Valley can simply pass through.

CONCLUSIONS

Has visibility changed significantly over the past 5 years? With such highly variable data, it is quite difficult to confidently establish trends over such a short time period. When the program began, the instrumentation then in use was the best available, i.e., state of the art. During the ensuing 5 years numerous changes (improvements in sensitivity, in particular) were made to the measurement equipment. Thus, the older nephelometry data are not as sensitive as the data collected today. The point that must be considered here is that any apparent trend in the data could be the result of (1) short term trends in meteorological conditions, (2) systematic measurement changes, (3) happenstance, (4) possible changes in light scattering, or (5) changes in light absorption admixed with possible changes in light scattering. These data represent the best estimates of light scattering (hence local visibility) available: no comparable long term "visibility" measurements exist elsewhere for comparison. This data base can be used to reach several conclusions about the current levels of visual air quality and the sources of visual air quality degradation.

Visibility at China Lake tends to be quite high.[4] Taking into account the scattering of light due to gases and estimating particle absorption at 20% of b_{sp}, the mean visibility is approximately 82 kilometers (51 miles), and the median, or 50% visibility, is 94 kilometers (58 miles).

Usable theoretical relationships between light, eye, target, and the atmosphere have been established that permit the calculation of the visual range at any time quickly and accurately.

In a clean atmosphere, such as at China Lake, a small increase in particulates will cause a large decrease in contrast or visibility.[7,13] While in a relatively dirty atmosphere that same increase in particulates may not be perceptible.

Comparisons of the 5-year particle scattering measurements indicate that significant variations in visibility occur on a diurnal, seasonal, and annual basis.

Quantification of atmospheric haziness can be accomplished by using nephelometry. Conclusions and generalizations from this procedure should, however, be made in light of the limitations of the instrument.

The nephelometry data base is continuing and expanding. A second nephelometer was installed in May 1980, and there are plans to install a third instrument. With the addition of these instruments it is feasible to explore the relative effects of regional and local haze and their respective contributions to the aerosol load.

[13] W. E. K. Middleton. *Vision Through the Atmosphere*. Toronto, University of Toronto Press, 1952.

Appendix A

VISION THROUGH THE ATMOSPHERE

ATTENUATION OF LIGHT BY THE ATMOSPHERE

Several factors determine how far one can see through the atmosphere. Generally these factors include optical properties of the atmosphere, amount and distribution of light, characteristics of the objects observed, and properties of the human eye.[13]

The human ability to see through the atmosphere is dependent on the concentration of particles (aerosols)* and gases suspended in the atmosphere. These particles and gases, which have the ability to scatter and absorb light, can cause the appearance of haze, a decrease in contrast, and a change in the perceived color of distant objects.**,[5]

CONTRAST RATIO

Man perceives objects by their contrast with the surroundings. The contrast can be attributed to the color and/or brightness of the object compared with its background. To permit calculations of visibility, valuable theoretical relationships have been established between light, eye, target, and the atmosphere.

The relationship between daytime target brightness and horizon brightness can be expressed as a contrast ratio. An object's initial contrast (its contrast at zero distance) can be defined as the ratio of object brightness minus horizon brightness divided by horizon brightness, or:

$$\underset{\text{(no dimensions)}}{\text{contrast ratio}} = \frac{\text{object brightness} - \text{horizon brightness}}{\text{horizon brightness}} \qquad \text{(A-1)}$$

For ordinary daytime conditions, brightness levels are usually between 1 and 1,000 or more foot-lamberts.

*Aerosol is a collective term for particulate matter suspended in the atmosphere.

**Scattering is distinguished from pure absorption in that the radiation (in this case light) in encountering a "scatterer" is not lost, but merely redirected, while with absorption, the radiation actually disappears as such only to be converted into heat.

If one assumes a black target viewed against the horizon sky in the daytime, the contrast (in this case unity) that the target would present to an observer standing directly in front of it would be caused by the apparent brightness of the horizon sky. (Remember that no light is emitted or reflected by a perfectly black object.) According to this definition, an absolutely black target, $B_t = 0$, in front of any background not absolutely black produces a contrast of minus unity, or $C = -1$. On the other hand, a non-black target in front of an absolutely black background assumes a contrast of plus infinity, or $C = +\infty$. Therefore, dark targets in front of light backgrounds, which represent general daytime visibility conditions, have contrasts ranging from 0 to -1, whereas light targets in front of dark backgrounds (nighttime conditions) have contrast ranging from 0 to $+\infty$. We will, for the sake of convenience, ignore the negative sign of the dark contrast and consider its absolute magnitude only.[14]

THRESHOLD CONTRAST

The lowest visually perceptible brightness contrast is called the liminal contrast or threshold contrast. The threshold contrast has been the object of considerable interest since it determines the maximum distances at which various components of a scene can be discerned. Laboratory experiments indicate that for most daylight viewing conditions, contrast ratios as low as 0.018 to 0.03 are perceptible. Typical observers can detect a 0.02 or greater contrast between large, dark objects and the horizon sky.[5] For the remainder of this report a threshold contrast value of 2% ($C = 0.02$) will be used for visual range calculations.

CONTRAST AND VISUAL RANGE

As distance increases from the observer to the object and horizon, the object begins to approach the brightness of the horizon. Thus, the contrast of an object relative to the horizon decreases.

In 1952 Middleton expressed contrast (C) as a function of observer and object distance.[13]

$$C = C_o e^{-b_{ext} x} \tag{A-2}$$

where

C_o = initial object contrast at zero distance

e = base for natural logarithms

b_{ext} = extinction coefficient (represents the fraction of light that is attenuated per unit distance as a light beam traverses the atmosphere)[3]

x = observer object distance.

[14] Hans Neuberger. *Introduction to Physical Meteorology*. University Park, Pa., Pennsylvania State University, 1967.

EXTINCTION COEFFICIENT

The extinction coefficient (also called the attenuation coefficient) is derived from the sum of the scattering coefficient (b_{scat}) and the absorption coefficient (b_{abs}). The ability of the atmosphere to scatter light is proportional to the scattering coefficient, while the absorption coefficient represents the atmospheric light absorbing abilities. The extinction coefficient (b_{ext}) is commonly expressed in a reciprocal length unit such as inverse meters (m^{-1}).

Equation A-2 shows that for all reasonable values of b_{ext}, contrast decreases with distance. The parameter that relates contrast to distance is the extinction coefficient, a somewhat misleading but well-established term. The extinction coefficient is a measure of the atmosphere's ability to attenuate image-forming light as it passes through the atmosphere from the scene to the observer. It is often preferable to discuss visibility in terms of extinction coefficient rather than visual range because the extinction coefficient can be linearly subdivided into contributions from various atmospheric components. These components will be discussed later.

KOSCHMIEDER RELATIONSHIP

Equation A-2 can be solved for the distance at which a black object has a standard 0.02 contrast ratio against a white background. When the contrast in Eq. A-2 becomes the threshold contrast, the distance becomes the visual range. If $C = 0.02$ and $C_o = 1.0$ then

$$0.02 = (1.0)e^{-b_{ext}x}$$

and

$$\ln(0.02) = -b_{ext}x$$

therefore

$$x = \frac{3.912}{b_{ext}} \tag{A-3}$$

with x and b_{ext} in similar units (i.e., x in meters and b_{ext} in inverse meters).*

Thus, visual range can be expressed as an extinction coefficient (b_{ext}) or a distance (x). If the extinction coefficient is measured along a sight path, then x is the visual range. If the extinction coefficient is measured at a point, then x is taken to be the local visual range. The two values of x are equal in a homogeneous atmosphere.[8] Figure A-1 shows the reciprocal relationship of the extinction coefficient to visual range. Equation A-3 states that visual range is now only a function of the extinction coefficient, and is inversely proportional to it. Thus, we have visibility as a measure of air quality.

The Koschmieder equation (Eq. A-3) provides an accurate formula for calculating visual range along a horizontal path. The derivation of the formula is based on certain assumptions

*Koschmieder equation (Eq. A-3) taken from Ref. 13.

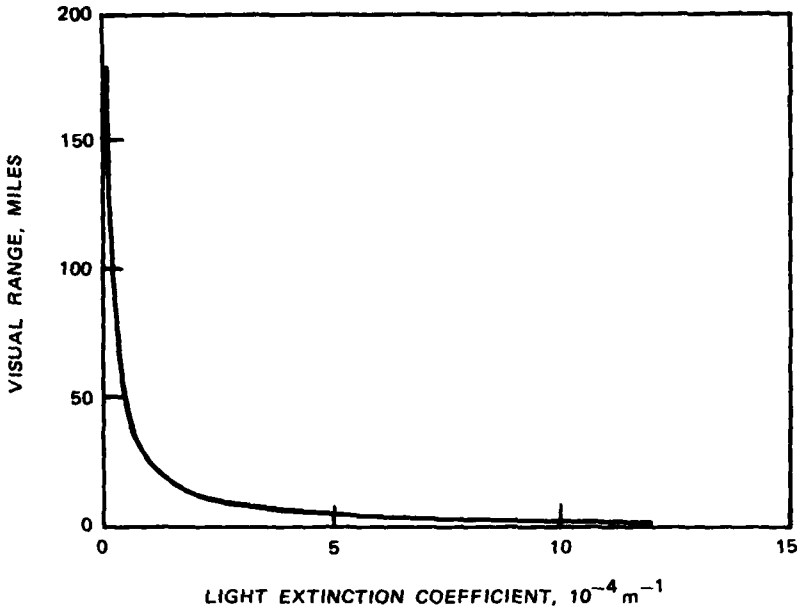

FIGURE A-1. Relationship of Extinction Coefficient to Visual Range (Koschmieder Relationship).

about atmospheric conditions and the psychology of human perception. The fundamental assumptions are

1. A perfectly black object (one that reflects no light) is perceived against an ideal white background.

2. An observer can detect a contrast ratio of 0.02 (the threshold contrast).

3. The atmosphere is homogeneous such that scattering and absorption of radiation are the same everywhere.

4. Sky brightness is the same at the object, the background, and the observer (cloudless sky).

5. The viewing distance is horizontal and the earth's curvature is ignored.

LIMITATIONS TO THE KOSCHMIEDER RELATIONSHIP

It should be noted that the visual range for nonblack targets strongly depends upon the initial contrast ratio, which in turn depends on color, angle, and intensity of illumination. To maximize object visibility the object should be of such a color as to have maximum contrast

relative to the background, and the observation should be made at wavelengths that maximize transmission between observer and object.*

For slant visual paths looking upward or downward, it is possible in principle to calculate the spectral radiance of target and background and to predict target contrast; but in real situations this often requires information such as color and reflectivity versus angle of the object, spectral radiance of background viewed from object location, and illumination on the object. These data are seldom available. Figure A-2 graphically presents other limitations to the Koschmieder relationship.

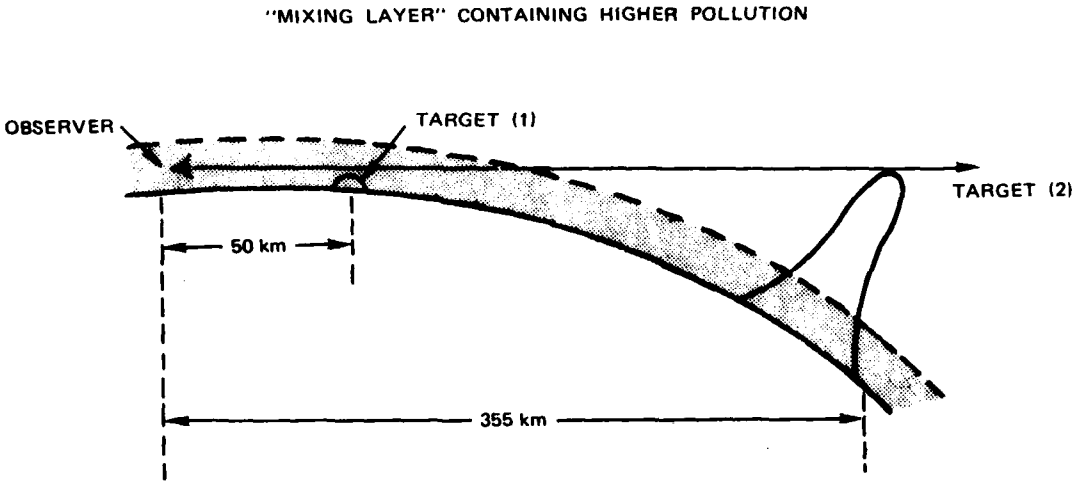

a. When visual range is short (Target 1), extinction and illumination through sight path is uniform. When true visual range is high (Target 2), Koschmieder equation underestimates visual range because extinction decreases with altitude, and illumination (sun angle) at target is different from that at observer (dimensions and earth's curvature exaggerated for clarity).[5]

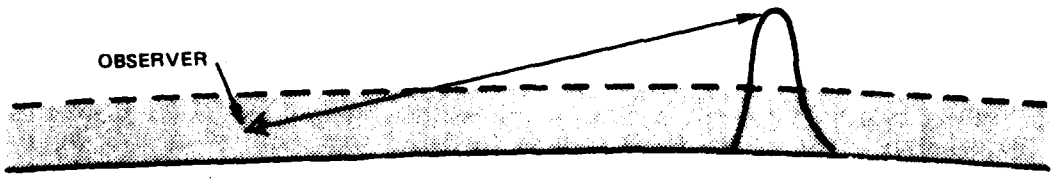

b. When viewing angle is not horizontal, extinction through the sight path is nonuniform. Koschmieder equation will underestimate visual range.[5]

FIGURE A-2. Limitations of Koschmieder Relationship.

*Personal communication with A. P. Waggoner, University of Washington, 1980.

The alteration of appearance of distant objects is thus controlled by the extinction of light in the atmosphere, mathematically stated as extinction coefficent, b_{ext}. To the extent that b_{ext} varies with wavelength, this alteration of appearance includes changes in the coloration of distant objects as well as their contrast.

So far visiblity, or visual range, has been expressed quantitatively as the distance at which an observer can detect a perfectly black object against a white background (0.02 contrast ratio). The extinction coefficient was introduced, visual range was related to it with a number of assumptions, and the major assumptions were briefly discussed. The extinction coefficent, however, is actually the summation of the four quantities shown in the following expression:[5]

$$b_{ext} = b_{Rg} + b_{sp} + b_{ag} + b_{ap}$$

where

b_{Rg} = scattering of light due to gases
b_{sp} = scattering of light due to particles
b_{ag} = absorption of light due to gases
b_{ap} = absorption of light due to particles

Each of these quantities has an inherently different wavelength dependence, as will be discussed later.

COMPONENTS OF THE EXTINCTION COEFFICIENT

Scattering of Light

Rayleigh Scatter, b_{Rg}. Lord Rayleigh (1899), in finding an explanation of the blue sky, observed that the sky is bluest when the air is purest and correctly referred the color to its actual cause, scattering of sunlight by the molecules of permanent gases of which the air is composed. Rayleigh demonstrated that an atmosphere containing only the primary gases scatters light in proportion to the inverse fourth power of the wavelength. This ideal atmosphere is frequently referred to as the Rayleigh atmosphere. At sea level the Rayleigh atmosphere has an extinction coefficient of approximately $13.2 \times 10^{-6} m^{-1}$ at 0.520 micrometer wavelength, limiting visibility to about 296 kilometers (184 miles).

Rayleigh scattering decreases with altitude and is proportional to air density; hence, at 0.520 microns wavelength

Altitude above sea level, feet (meters)		b_{Rg} at 0.520 micron, $X10^{-6}m^{-1}$
0	(0)	13.2
3,281	(1,000)	11.4
6,562	(2,000)	10.6
9,843	(3,000)	9.7
13,124	(4,000)	8.8

Rayleigh scatter thus amounts to a simple, definable and measurable background level of extinction against which other extinction components (e.g., man-made pollutants) can be compared.[5]

Particle Scatter, b_{sp}. Visibility reduction at China Lake is dominated by the scattering of light due to particles in the atmosphere.[7] It is evident that scatter is greatly increased by the haze and dust particles in the air, particularly in the forward direction. As the particle concentration increases from very low levels where Rayleigh scatter dominates, b_{sp} increases until eventually b_{sp} equals b_{Rg}. At this point the visual quality of air is controlled by particle scattering.

An important parameter that characterizes the pattern of light scattering by a particle is the ratio of the particle diameter to the wavelength of visible light. Visible light that affects the retina of the human eye has a bandwidth of approximately 0.40 to 0.70 microns. Light of such wavelengths is affected by particles of various sizes. Large particles (several microns in diameter) will scatter light by three fundamental processes; reflection, diffraction, and refraction. These three processes cause light to deviate from its original direction of travel (forward direction). Most of the light scattered by large particles is only slightly altered from the forward direction; thus, when facing the sun the air appears white.

When a scattered light beam strikes another particle it is scattered (secondary scattering), and scattered again, and so on (multiple scattering). In the case of sunlight passing through the atmosphere, all the particles that make up the atmosphere will send scattered light in all directions so that the atmosphere itself appears luminous. This is called airlight.

For particles approximately the diameter of the wavelength of light, a greater proportion of the incident light will be scattered away from the forward direction. Calculations show that most of the scattered light is deflected by more than 1 degree, but less than 45 degrees from the forward direction. The light scattered from these particles, as from the larger particles, is essentially white. Figure A-3 notes this phenomenon.

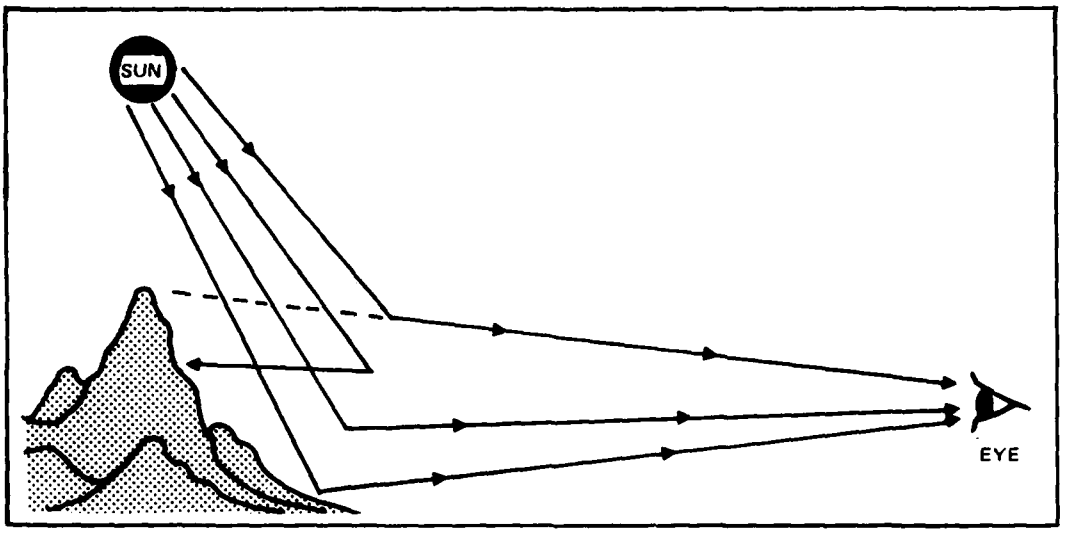

a. Looking toward sun (haze appears brighter) forward scatter obscures view of distant mountain.

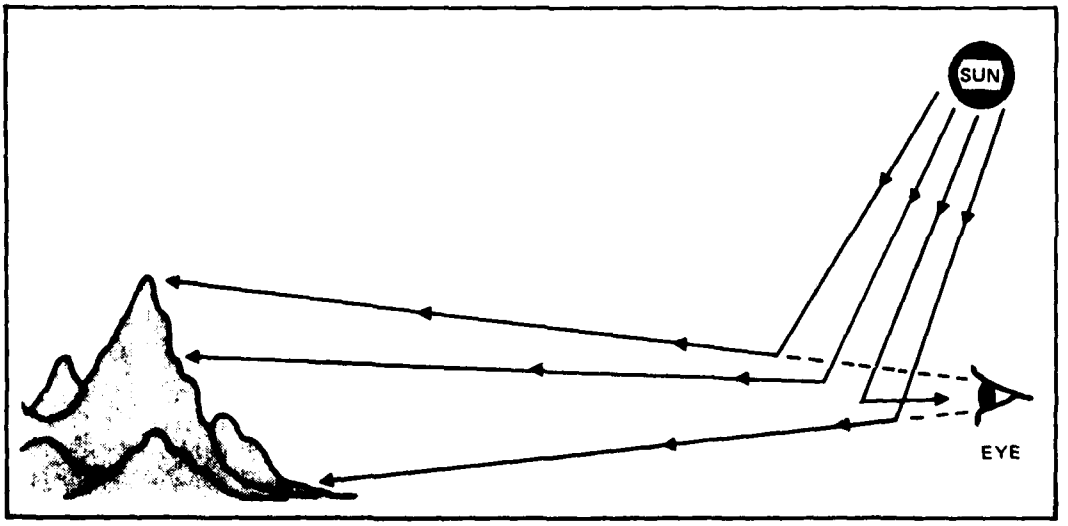

b. Sun behind observer (haze is less bright) backward scatter, being less than forward scatter, does not obscure view as effectively.

FIGURE A-3. Effect of Sun Angle on Visibility.

Particles less than 0.1 micron in diameter scatter light equally in the forward and backward directions and only slightly less from the sides. Small particles scatter more light in the short wavelength (blue) than in the long wavelength (red).

Particle size is the most important parameter in relating particle mass concentration and particle scattering. Particles in the 0.2 to 1.0 micron range are most efficient at scattering natural sunlight (see Figure A-4). The particle size distribution of the lower atmosphere also has certain regular features. Usually there are two volume modes, a fine mode centered at approximately 0.3 microns and coarse mode centered at 5 to 30 microns. The two modes are usually uncoupled in that they have different sources, lifetimes, and removal mechanisms. The peaking of scattering at 0.3 microns combines with the measured peak in volume at 0.3 microns so that the fine particles dominate extinction in almost all cases.

The addition of small amounts of fine particles (less than 1.0 micron) throughout the viewing distance tends to whiten the horizon sky making distant dark objects and intervening air light appear more grey. Particles generally scatter more light in the forward direction than in other directions; thus, haze appears bright in the forward-scatter mode and dark in the backscatter mode (see Figure A-3). This is due to the dependence on illumination angle.

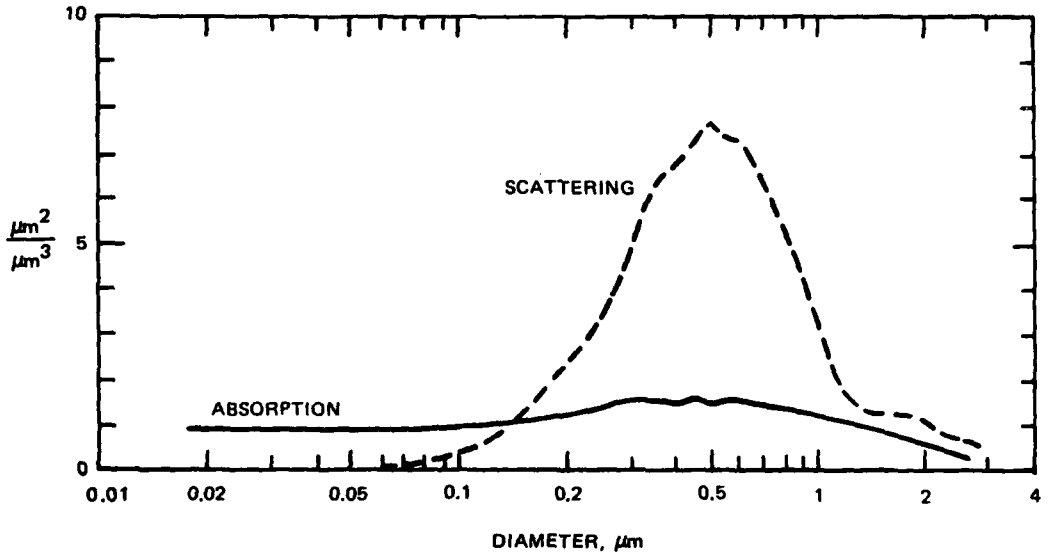

FIGURE A-4. Single Particle Scattering and Absorption. For a single particle of typical composition the scattering per volume has a strong peak at particle diameter of 0.5 μm. The absorption per aerosol volume, however, is only weakly dependent on particle size. Thus the light extinction by particles with diameters less than 0.1 μm is primarily due to absorption.[6] Scattering for such particles is very low. A black plume of soot from an oil burner is a practical example.

Absorption of Light

Gas Absorption, b_{ag}. Nitrogen dioxide (NO_2) is the only light absorbing gas present in optically significant quantities. Nitrogen dioxide and its precursor, nitric oxide (NO), are emitted by high temperature processes such as those used in fossil fuel power plants. NO_2 absorbs light selectively and is strongly blue-absorbing; it will color plumes red, brown, or

yellow. Nitrogen dioxide is often described as being the color of whiskey; its hue and intensity of color depend on concentration, optical path length, aerosol properties, and conditions of illumination. Almost all of the nitrogen oxide emitted from combustion is NO, a colorless gas; however, chemical reactions in the atmosphere can oxidize a substantial portion of the colorless NO to reddish brown NO_2. Nitrogen dioxide seems to be important only in plumes, not in a well mixed layer or regional haze. Figure A-5 shows the wavelength dependency of Rayleigh scattering.

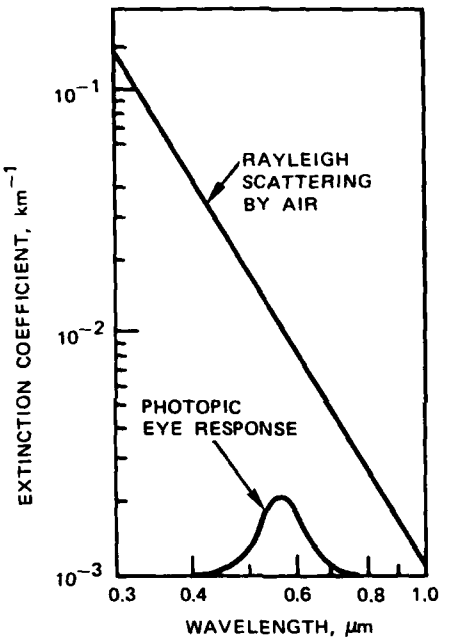

FIGURE A-5. Rayleigh Scattering by Air, b_{Rg}, is Proportional to λ^{-4}; Reduced Density at Higher Altitudes Causes a Reduction of b_{Rg}.

Particle Absorption, b_{ap}. In the past, particle absorption of light was thought to be insignificant. Recent work, however, seems to indicate otherwise.[8] The amount of particle absorption depends on the composition and size distribution of the particles. The most important contributor to absorption appears to be graphitic carbon (in the form of soot). The source of this highly absorbing submicrometer-size soot appears to be the combustion of liquid fuels, particularly in diesel engines; coal combustion may not be a major contributor.

The effects of particle absorption on the extinction coefficient vary. In "clean" areas b_{ap} can be 10% or less of b_{sp}. In urban areas b_{ap} can reach 50% of b_{sp} or greater. Some measurements at China Lake indicate ratios of 22% b_{ap} to b_{sp}. (It should be noted that this report uses particle absorption approximations of 20% in the visual range calculations.)

SUMMARY

In this appendix vision through the atmosphere has been examined. The term visual range has been defined as the distance at which an observer would just be able to discern a perfectly black object against an ideally white background (0.02 contrast), and visual range has been related to an extinction coefficient via the Koschmieder relationship. Further, four linearly additive components of this light extinction coefficient have briefly been considered. Of the four components, particle scattering plays the major role in visibility reduction at China Lake.

INITIAL DISTRIBUTION

3 Naval Air Systems Command
  AIR-00D4 (2)
  AIR-03P1 (G. W. Leonard) (1)
2 Naval Sea Systems Command (SEA-99612)
1 Consolidated Civilian Personnel Office, U.S. Naval Activities, U.K. (N. Curran)
1 Army Environmental Hygiene Agency, Aberdeen Proving Ground (D. Guzewich)
1 Air Force Rocket Propulsion Laboratory, Edwards Air Force Base (6510 ABG/DEEV, J. Baker)
1 Air Force Rocket Propulsion Laboratory, Edwards Air Force Base (P. Brady)
12 Defense Technical Information Center
1 Dryden Flight Research Center (NASA), Edwards Air Force Base (V. Horton)
1 Air Resources Board, Sacramento, CA (Dr. J. Suder)
1 Archaeological Research Unit, Riverside, CA (Dr. P. Wilke)
1 Assistant City Administrator, Oceanside, CA (D. Duckworth)
2 California Air Resources Board, El Monte, CA
  J. Wendt (1)
  K. J. Torre (1)
1 California Air Resources Board, Sacramento, CA (R. Tuvell)
1 Charter Data Processing, Healdsburg, CA
1 Chevron Research Company, Richmond, CA (Dr. J. Ouimette)
1 Clarence Shields Associates, Fernley, NV
1 Death Valley National Park Research Management Specialist, Death Valley, CA (P. Sanchez)
1 Great Basin Unified Air Pollution Control District, Bishop, CA (C. Fryxell)
1 Kern County Air Pollution Control District, Bakersfield, CA (L. Landis)
1 Kerr-McGee Corporation, Trona, CA (Environmental Director, J. Smith)
1 Meteorology Research, Inc., Altadena, CA (W. Wilson)
1 San Bernardino County Air Pollution Control District, San Bernardino, CA (W. Mook)
1 Santa Barbara Research Center, Goleta, CA (J. Socolich)
1 Santa Fe Research Corporation, Santa Fe, NM (Dr. J. Trijonis)
1 University of California (Department of Earth Sciences), Riverside, CA (F. Kuykendall)
1 University of Washington (Department of Civil Engineering), Seattle, WA (FC-05, Dr. A. P. Waggoner)
1 Washington University, St. Louis, MO (Dr. W. White)